Chinese Chemical Letters 31 (2020) 2507–2511

Contents lists available at ScienceDirect

Chinese Chemical Letters

journal homepage: www.elsevier.com/locate/cclet

Communication

A dense graphene monolith with poloxamer prefunctionalization enabling aqueous redispersion to obtain solubilized graphene sheets

Chen Ye[a,b], Fan Zhang[a,c], Xue Tan[a,b], Huifang Sun[a,c], Wen Dai[a,b], Ke Yang[a,b], Minghui Yang[d], Shiyu Du[e], Dan Dai[a,b], Jinhong Yu[a,b], Nan Jiang[a,b], Weitao Su[f], Li Fu[f], He Li[a,b,*], Jing Kong[g,**], Cheng-Te Lin[a,b,*]

[a] Key Laboratory of Marine Materials and Related Technologies, Zhejiang Key Laboratory of Marine Materials and Protective Technologies, Ningbo Institute of Materials Technology and Engineering, Chinese Academy of Sciences, Ningbo 315201, China
[b] Center of Materials Science and Optoelectronics Engineering, University of Chinese Academy of Sciences, Beijing 100049, China
[c] Faculty of Materials Science and Engineering, Kunming University of Science and Technology, Kunming 650093, China
[d] Ningbo Institute of Materials Technology and Engineering (NIMTE), Chinese Academy of Sciences, Ningbo 315201, China
[e] Division of Functional Materials and Nanodevices, Ningbo Institute of Materials Technology and Engineering, Chinese Academy of Sciences, Ningbo 315201, China
[f] College of Materials and Environmental Engineering, Hangzhou Dianzi University, Hangzhou 310018, China
[g] Department of Electrical Engineering and Computer Science, Massachusetts Institute of Technology, Cambridge, Massachusetts 02139, United States

ARTICLE INFO

Article history:
Received 3 December 2019
Received in revised form 6 January 2020
Accepted 8 January 2020
Available online 8 January 2020

Keywords:
Dense monolith
Graphene sheets
Poloxamer
Aqueous redispersion
Surface functionalization

ABSTRACT

The realization of good aqueous dispersibility of commercial graphene products composed of exfoliated graphene sheets is of significance for downstream applications. However, the tap density of commercial graphene powder is quite low (0.03–0.1 kg/m^3), meaning that 1 kg graphene powder occupies about 10–30 m^3 in volume during transportation. And, the available content of commercial graphene dispersion/slurry in aqueous medium cannot exceed 5 wt%, although the density is high (≈ 1050 kg/m^3). In this work, a graphene monolith was prepared by oven-drying of graphene sheets prefunctionalized with poloxamer surfactants. Our graphene monoliths not only have a high density (1500 kg/m^3) and high graphene content (≈ 10 wt%), but also a full capability to be completely redispersed (≈ 100%) in water by bath sonication to obtain solubilized graphene sheets, whose lateral size and thickness are unchanged compared to as-exfoliated ones. Moreover, a simple empirical method was proposed to predict the redispersion capability of graphene monoliths using different poloxamers by contact angle measurements. Our results provide a universal approach to make exfoliated graphene-based products with better downstream availability and lower transportation cost.

Graphene, a well-known two-dimensional material, exhibits interesting properties different from other nanomaterials and has attracted considerable attention in both academia and industry [1–3]. Made up by one-atom-thick honeycomb-latticed carbon atoms, graphene has many fascinating properties, including highest thermal conductivity [4], ultrahigh carrier mobility [5], great mechanical strength, *etc.* [6], thus showing great application potential in conductive inks [7], functional polymer composites [8,9], energy storage/conversion [10–12], and flexible transparent electronics [13,14]. In order to better develop graphene based applications, the production of graphene in a large quantity or large-area using high-efficiency, low-cost, and environmentally friendly methods is strongly demanded. In the past ten years, graphene production has been successfully commercialized based on top-down and bottom-up approaches, the former typically including Hummers method [15], electrochemical exfoliation [16] and sonication-assisted liquid exfoliation [17], as well as the latter mainly chemical vapor deposition (CVD) [18]. Graphene products prepared by above two approaches have different features and suitable applications, as an example, large-area graphene films grown by CVD are good candidates for use in transparent conductive electrodes [19]. In addition, exfoliated graphene sheets

* Corresponding authors at: Key Laboratory of Marine Materials and Related Technologies, Zhejiang Key Laboratory of Marine Materials and Protective Technologies, Ningbo Institute of Materials Technology and Engineering, Chinese Academy of Sciences, Ningbo 315201, China.
** Corresponding author.
E-mail addresses: lihe@nimte.ac.cn (H. Li), jingkong@mit.edu (J. Kong), linzhengde@nimte.ac.cn (C.-T. Lin).

https://doi.org/10.1016/j.cclet.2020.01.021
1001-8417/

with a production capacity of several hundred kilograms has been applied in anticorrosive paints [20,21], heat spreaders [22,23], and conductive additives for Li-ion batteries, *etc*. [24].

Due to the strong π-π interaction between graphene layers, exfoliated graphene sheets without appropriate treatment would be easily restacked and lose their properties during storage and transportation [25]. Therefore, the guarantee of good redispersibility of graphene products in a liquid medium (in most cases, water) is of most importance for further use. In general, commercial exfoliated graphene is made into two forms: liquid dispersion/slurry and dry powder [26]. The liquid dispersion/slurry is prepared by dispersing exfoliated graphene in aqueous or organic media and certainly has good dispersibility [27]. However, in order to avoid restacking, the available content of graphene in the dispersion/slurry is limited to be less than 5 wt% [28], suggesting very low volume usage of the products and high rise of transportation cost. In contrast, the powder form has a high content of graphene (50−90 wt%) [29], but a poor redispersibility without the assistance of surfactants, especially when dispersed in water [30]. Moreover, the tap density of graphene powder obtained mostly by spray drying is quite low (0.03–0.1 kg/m^3) [31,32], meaning that 1 kg graphene powder occupies about 10–30 m^3 in volume. This results in low transportation efficiency due to unnecessary waste of cargo space. As a result, currently, it has a real demand from the industry side to provide graphene products with the form which possesses good aqueous redispersibility, high packing density, and high graphene content.

Here, a dense monolith made of graphene sheets prefunctionalized with poloxamer nonionic surfactants was prepared by oven drying. Poloxamer is an effective and innocuous surfactant, and has been commonly used for improving water solubility and bioavailability of drugs [33]. Compared to as-prepared graphene, the oven dried monoliths made of poloxamer functionalized graphene sheets have a density of up to 1500 kg/m^3, which is four orders magnitude higher than the tap density of commercial graphene powder. Moreover, with the assistance of poloxamers (*e.g.*, Pluronic P123), the graphene monoliths can be completely redispersed in water by bath sonication for 5 min. Our investigation may offer an alternative concept to make products based on exfoliated graphene with better downstream availability and lower transportation cost.

In this work, the as-prepared graphene sheets were dispersed in deionized (DI) water medium with a concentration of 0.03 mg/mL. Poloxamers with different mass ratios of surfactant/graphene were dissolved in 10 mL graphene dispersion, respectively, by ultrasonication for 2 h. The solutions were dried in the oven at 120 °C for 3 h to completely remove water. Then graphene powder was obtained, following with cold-molding into monolith. As well known, due to the attractive van der Waals interactions between graphene sheets, exfoliated graphene without hydrophilic surface functionalization tend to form aggregates in aqueous medium [34]. In such cases, as presented in Fig. 1a, the oven dried monoliths made of unfunctionalized graphene sheets cannot be well redispersed in water, because of the creation of a high binding energy ($\approx$ 1.65 eV/nm^2) between graphene interlayers during drying [35,36]. In contrast, with the assistance of enough surfactants, graphene sheets can be homogeneously redispersed from the monolith by bath sonication for 5 min. This interprets the significance of our study to produce water redispersible graphene monoliths by functionalization with poloxamer surfactants.

Graphene sheets used in this study were synthesized using an electrochemical exfoliation method [37], by which the obtained sheets are composed of few-layer graphene with a lateral size ranging from a few to more than 10 μm (Fig. 1b). The characteristic of electrochemically exfoliated graphene is the better electrical properties without the need of further reduction treatment [38],

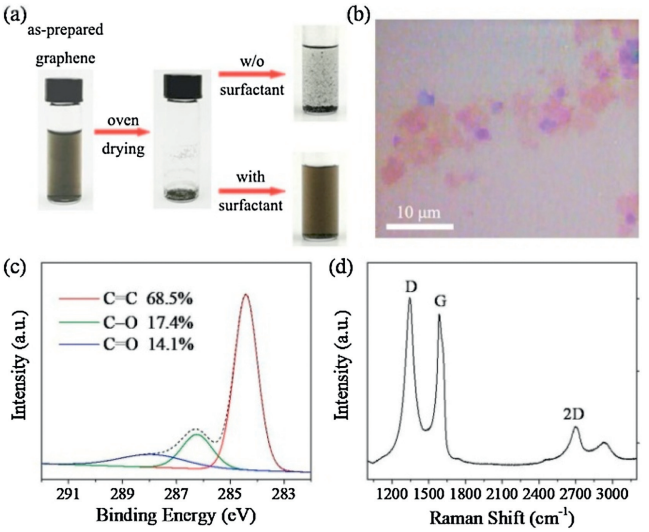

Fig. 1. (a) Schematic of water redispersible graphene monoliths with the assistance of poloxamer surfactants. (b) Morphology, (c) C 1s XPS spectrum and (d) Raman spectrum of electrochemically exfoliated graphene sheets.

but the intrinsic hydrophobic feature makes it difficult to disperse in water due to the low content of surface oxygen-containing groups. As the high-resolution C 1s XPS spectrum shown in Fig. 1c, three deconvoluted components can be assigned to sp^2-hybridized bonds (C=C, at $\approx$ 284.4 eV), hydroxyl (C—O, at $\approx$ 286.1 eV), and carbonyl groups (C=O, at $\approx$ 287.1 eV), respectively [39]. Accordingly, the ratio of oxygen-containing groups of electrochemically exfoliated graphene is $\approx$ 31.5%, which is lower than that of graphene oxide (46.5%–57.2%) [40]. In addition, a 2D-band at $\approx$ 2700 cm^{-1} with a I_{2D}/I_G ratio of 0.31 (the peak height ratio between 2D- and G-bands) can be found in the Raman spectrum in Fig. 1d, demonstrating that the quality of electrochemically exfoliated graphene is close to reduced graphene oxide [41,42].

Not only the good aqueous dispersibility, but the maintenance of atomic thickness of graphene redispersed from the monolith is also of importance for further applications. The influence of graphene sheets prefunctionalized with and without poloxamers on their morphology after redispersion was investigated, as exhibited in Fig. 2. In Fig. 2a, the as-prepared graphene sheets placed on SiO_2/Si substrate (300 nm-thick SiO_2) show a typical polygonal shape, and the restacking phenomenon can be clearly seen in Fig. 2b when graphene was oven dried without the use of surfactants and then redispersed in water by ultrasonication. In contrast, Fig. 2c indicates that the morphology of redispersed graphene sheets with poloxamer functionalization is as same as that of as-prepared one. The change of the sample thickness was precisely examined by AFM analysis, as the results displayed in Figs. 2d–f. Note that the samples were rigorously rinsed by DI water to remove the surfactant residue before AFM measurements [39]. As expected, the morphological variation between three samples according to AFM images confirms the SEM observations. Fig. 2g is the statistical analysis of graphene thickness derived from Figs. 2d–f, demonstrating that the average thickness of redispersed graphene with functionalization (5.9 nm) is similar to that of as-prepared one (5.0 nm), whereas, without surfactant assistance, graphene sheets would be restacked and difficult to be well redispersed based on the increased thickness (25.4 nm). Fig. S1 (Supporting information) indicates that the Raman spectrum of the poloxamer-prefunctionalized graphene is similar to that of pristine as-prepared graphene sheets, interpreting that the surface functionalization of graphene sheets may not alter their defect degree and crystalline structure. In contrast to as-prepared

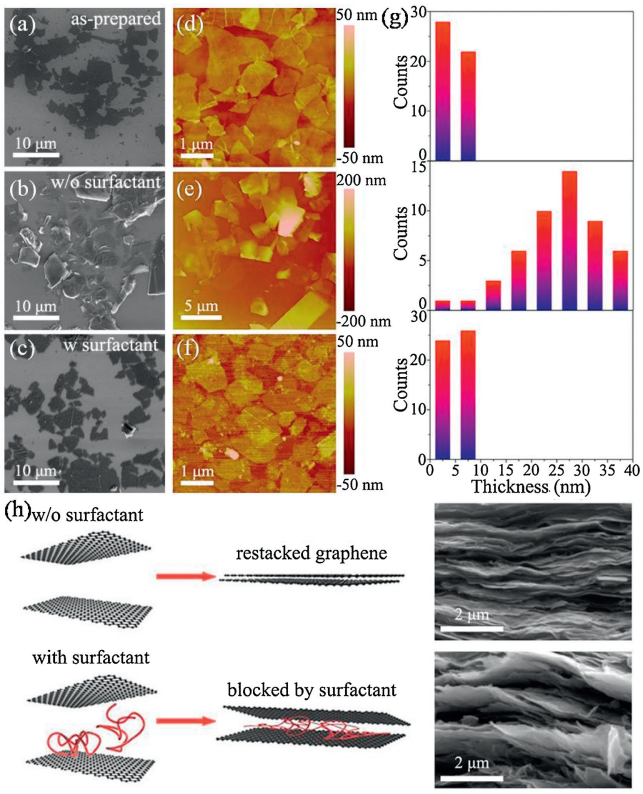

Fig. 2. SEM images of (a) as-prepared graphene sheets and the samples redispersed from the monolith (b) without and (c) with poloxamer functionalization. (d–f) The corresponding AFM images. (g) Statistical analysis of graphene thickness derived from (d–f). (h) Schematic of the function of surfactants for improving the redispersibility of graphene monoliths.

graphene sheets, a dominant C—O peak at ≈ 285.8 eV in C 1s XPS spectrum can be observed for the sample after poloxamer prefunctionalization (Fig. S2 in Supporting information), which can be attributed to the contribution from rich ether bonds of poloxamer molecules. As shown in Fig. 2h, the enhancement mechanism of water redispersibility of graphene monoliths with functionalization can be attributed to the blocking effect of surfactants between graphene interlayers. In addition, during redispersion, the dissolved surfactants may also lower the surface tension of water to better match that of graphene [43].

In order to systematically study the redispersion effect based on the conditions of surfactants, four kinds of poloxamer surfactants with a general term of poly(ethylene oxide)–poly(propylene oxide)–poly(ethylene oxide) triblock copolymers (PEO–PPO–PEO) were employed (Pluronic F68, L61, F127 and P123). In Fig. 3a, we found that the redispersion capability of graphene sheets was improved by increasing the added amount of poloxamers in the graphene monoliths. The monoliths with a similar density of ≈ 1500 kg/m^3 were prepared by mixing water dissolved poloxamer with 0.01–3 mg/mL concentrations and 0.03 mg/mL graphene, followed by oven drying. The redispersion properties of graphene monoliths can be quantitatively characterized by determining the absorbance of redispersed solution in the UV–vis spectra. A calibration curve was first developed by dispersing as-prepared graphene with defined concentrations in ethanol, and the absorbance in the UV–vis region was recorded as presented in Fig. 3b. Since there is no absorption peak of the dispersion in the visible light range of 400–800 nm, the absorbance at 650 nm wavelength was set as an indicator of dispersed/redispersed graphene concentration (mg/mL) and the calibration curve could be defined as: Y(absorbance at 650 nm) = 30.1 X(graphene concentration). The linearity of the calibration curve suggests a good fit of Beer–Lambert law [44]. As shown in Fig. 3c, no matter what kind and amount of poloxamers were added, the UV–vis absorbance of as-prepared graphene dispersions keeps almost the same. However, after drying, the absorbance of graphene inks redispersed from the monolith varies as a function of added poloxamer concentration (0.01–3 mg/mL). This indicates that graphene sheets could be uniformly separated from the monolith and the surface tension of water could be adjusted to an appropriate value, when enough surfactants were added. Note that excess surfactants would not give a bonus to help redispersion.

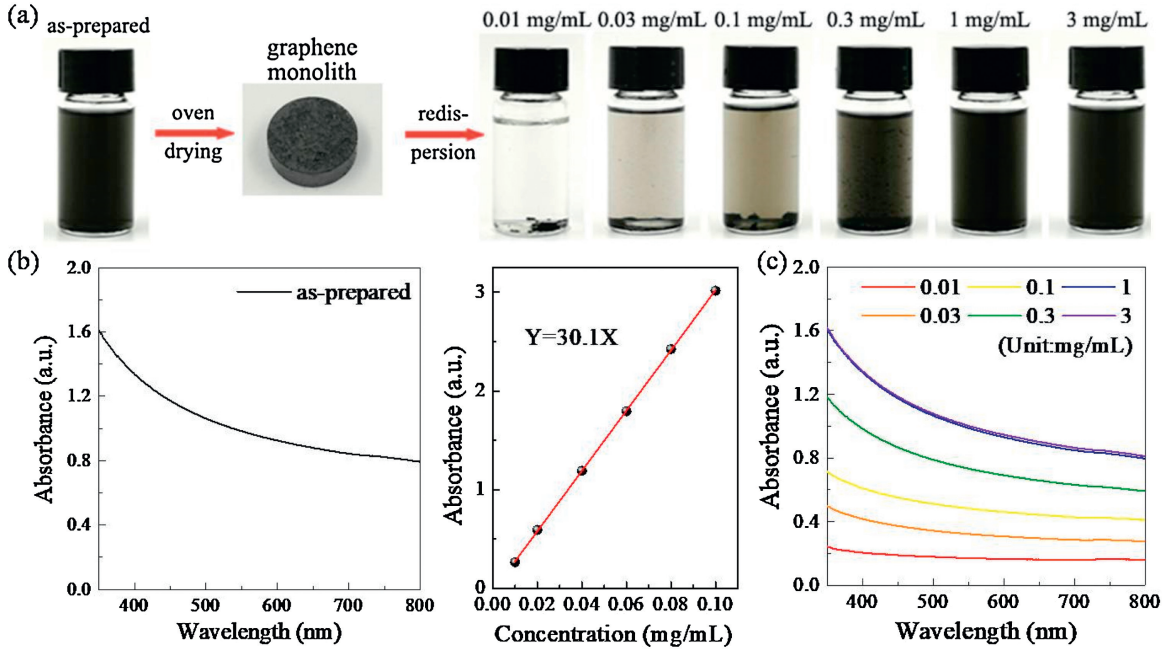

Fig. 3. (a) Photos of as-prepared graphene dispersion and redispersed graphene inks with different poloxamer concentrations. (b) UV–vis absorbance of as-prepared graphene dispersions and the calibration curve. (c) UV–vis absorbance of redispersed graphene inks with different poloxamer concentrations.

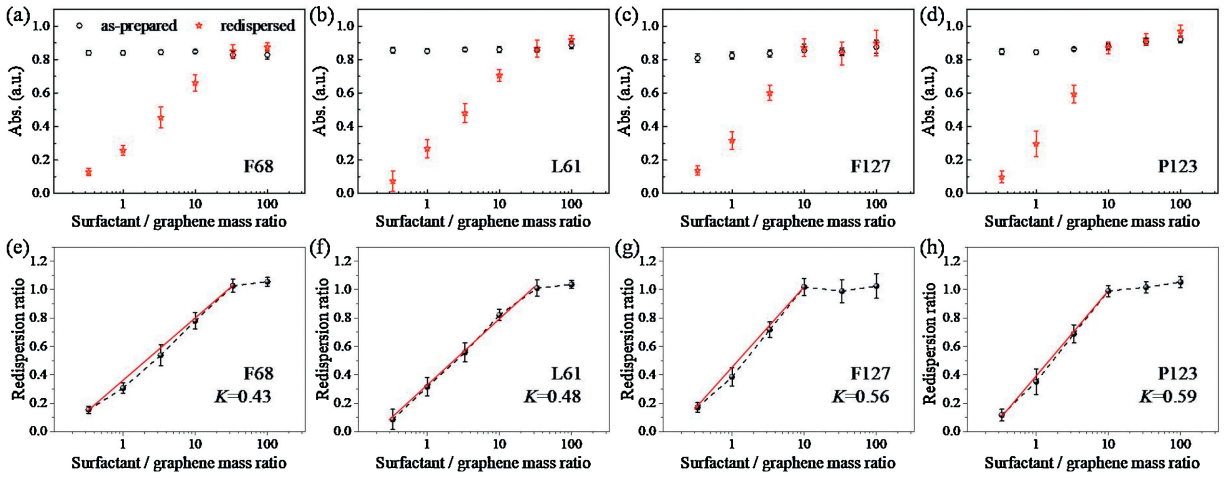

Fig. 4. (a–d) UV–vis absorbance at 650 nm of as-prepared graphene dispersions and redispersed graphene inks with different poloxamer conditions. (e–h) The redispersion ratio and K value calculated from (a–d).

According to the value of UV–vis absorbance at 650 nm, the redispersion ratio of graphene inks from the monolith with different poloxamer conditions can be obtained for comparing their redispersion capability. In Figs. 4a–d, the absorbance is similar (≈ 0.85) for as-prepared graphene dispersions (graphene content: 0.03 mg/mL) with various poloxamer types and added concentrations. After redispersion, the absorbance of graphene inks is quite low (0.05–0.15) when only small amount of poloxamers was added at a mass ratio of surfactant/graphene of 0.33, and then linearly increases with an increase of the surfactant/graphene mass ratio, eventually achieving a saturation value (0.84–0.92) which is similar to that of as-prepared graphene dispersions. Due to the limited resolution of UV–vis spectrometer, some absorbance values of redispersion are over those of as-prepared dispersion. In Figs. 4e–h, the redispersion ratio can be estimated, which is defined as the ratio of absorbance at 650 nm between redispersed graphene ink and as-prepared graphene dispersion. Correspondingly, the *K* value calculated from the slope of linear fit is an indicator: a higher *K* represents easy achievement of 100% redispersion of graphene monoliths at a lower dosage of poloxamers. As a result, the estimated values are 0.43 (F68), 0.48 (L61), 0.57 (F127) and 0.60 (P123), respectively, demonstrating that P123 is the most effective surfactant for our purpose and the dosage is ≈ 90% compared to that of F68 for achieving complete redispersion.

The relation between *K* value and affinity between poloxamer and graphene was studied by contact angle measurements. As displayed in Fig. 5a, aqueous solution with 1 mg/mL poloxamer concentration was dropped onto the surface of as-prepared graphene sheets, and the observed contact angles are 54.2° (F68), 45.1° (L61), 41.2° (F127) and 31.7° (P123), respectively. At steady-state, the contact angle of those solution drops in Fig. 5a is less than 60.0°, indicating that graphene is lyophilic to poloxamer aqueous solution, whereas the contact angle is large (≈ 70.2°) when DI water was dropped on the graphene surface. As shown in Fig. 5b, we concluded that a better affinity (smaller contact angle) between poloxamer and graphene may lead to a higher *K* value. The redispersion mechanism of graphene monoliths with functionalization is proposed and schematically illustrated in Fig. 5c. During redispersion, water is difficult to insert into graphene interlayers due to the hydrophobic nature of graphene, and graphene sheets prefunctionalized with poloxamer result in ease of intercalation of water molecules because of low contact angle between them.

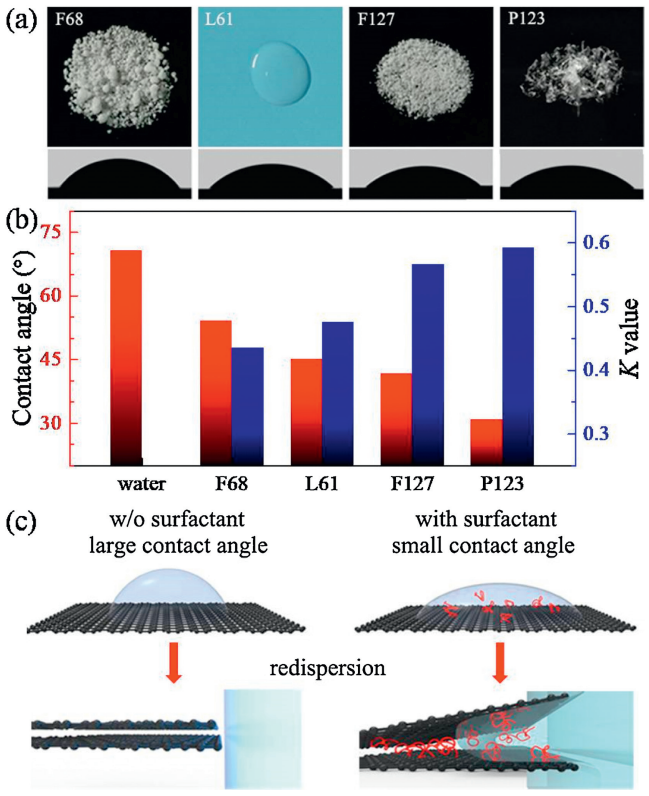

Fig. 5. (a) Contact angle measurements of poloxamer aqueous solutions dropped on the graphene surface. (b) *K* value as a function of contact angle. (c) The redispersion mechanism of graphene monoliths with poloxamer functionalization.

In summary, we have made a systematic study on the preparation of graphene monoliths which possesses good aqueous redispersibility (≈ 100%), high density (1500 kg/m^3), and high graphene content (≈ 10 wt%). The redispersibility of dense graphene monoliths is implemented by functionalization with poloxamer surfactants, such as Pluronic P123. Note that either the lateral size or sheet thickness of graphene would not be altered after redispersion based on our proposed approach, guaranteeing the convenience and performance of downstream applications. Moreover, we developed a simple empirical method to predict the redispersion capability of graphene monoliths using different

poloxamers by contact angle measurements. Note that this empirical finding may also be applied to other surfactant systems. Our work paves a feasible way to make water redispersible graphene products which may lower transportation cost and give better downstream availability.

Declaration of competing interest

The authors declare that they have no known competing financial interests or personal relationships that could have appeared to influence the work reported in this paper.

Acknowledgments

The authors are grateful for the financial support by the National Natural Science Foundation of China (Nos. 51573201, 51501209 and 201675165), NSFC-Zhejiang Joint Fund for the Integration of Industrialization and Informatization (No. U1709205), the Strategic Priority Research Program of the Chinese Academy of Sciences (No. XDA22000000), Scientific Instrument Developing Project of the Chinese Academy of Sciences (No. YZ201640), Science and Technology Major Project of Ningbo (Nos. 2016S1002 and 2016B10038), and International S&T Cooperation Program of Ningbo (No. 2017D10016) for financial support. We also thank the Chinese Academy of Sciences for Hundred Talents Program, Chinese Central Government for Thousand Young Talents Program, and 3315 Program of Ningbo.

Appendix A. Supplementary data

Supplementary material related to this article can be found, in the online version, at doi:https://doi.org/10.1016/j.cclet.2020.01.021.

References

[1] K.S. Novoselov, A.K. Geim, S.V. Morozov, et al., Science 36 (2004) 666–669.
[2] Q.L. Yuan, Y. Liu, C. Ye, et al., Biosens. Bioelectron. 111 (2018) 117–123.
[3] P.T.K. Loan, D. Wu, C. Ye, et al., Biosens. Bioelectron. 99 (2018) 85–91.
[4] A.A. Balandin, S. Ghosh, W. Bao, et al., Nano Lett. 8 (2008) 902–907.
[5] A.S. Mayorov, R.V. Gorbachev, S.V. Morozov, et al., Nano Lett. 11 (2011) 2396–2399.
[6] C. Lee, X. Wei, J.W. Kysar, et al., Science 321 (2008) 385–388.
[7] P.G. Karagiannidis, S.A. Hodge, L. Lombardi, et al., ACS Nano 11 (2017) 2742–2755.
[8] L. Lv, W. Dai, A. Li, C.T. Lin, Polymers 10 (2018) 1201–1210.
[9] H. Hou, W. Dai, Q. Yan, et al., J. Mater. Chem. A 6 (2018) 12091–12097.
[10] A.M. Gaikwad, A.C. Arias, D.A. Steingart, Energy Technol. 3 (2015) 305–328.
[11] X. Cao, C. Tan, M. Sindoro, et al., Chem. Soc. Rev. 46 (2017) 2660–2677.
[12] W. Shi, J. Mao, X. Xu, et al., J. Mater. Chem. A 7 (2019) 15654–15661.
[13] J. Liu, Y. Yi, Y. Zhou, H. Cai, Nanoscale Res. Lett. 11 (2016) 108–115.
[14] C.-M. Gee, C.C. Tseng, F.Y. Wu, et al., Displays 34 (2013) 315–319.
[15] L. Peng, Z. Xu, Z. Liu, et al., Nat. Commun. 6 (2015) 5716–5725.
[16] H. Sun, D. Chen, C. Ye, et al., Appl. Surf. Sci. 435 (2018) 809–814.
[17] R. Narayan, S.O. Kim, Nano Converg. 2 (2015) 20–39.
[18] T. Wu, Z. Liu, G. Chen, et al., RSC Adv. 6 (2016) 23956–23960.
[19] L. La Notte, E. Villari, A.L. Palma, et al., Nanoscale 9 (2017) 62–69.
[20] E. Šest, G. Dražič, B. Genorio, I. Jerman, Sol. Energy Mater. Sol. Cells 176 (2018) 19–29.
[21] W. Sun, L. Wang, Z. Yang, et al., Mater. Lett. 228 (2018) 152–156.
[22] Y. Chen, X. Hou, R. Kang, et al., J. Mater. Chem. C 6 (2018) 12739–12745.
[23] P.H. Lee, W.M. Tu, H.C. Tseng, IEEE Trans. Electron Devices 65 (2018) 352–355.
[24] L.H. Hu, F.Y. Wu, C.T. Lin, A.N. Khlobystov, L.J. Li, Nat. Commun. 4 (2013) 1687–1694.
[25] D.D.L. Chung, J. Mater. Sci. 37 (2002) 1475–1479.
[26] X. You, S. Yang, J. Li, et al., ACS Appl. Mater. Interfaces 9 (2017) 2856–2866.
[27] U. Khan, A. O'Neill, M. Lotya, S. De, J.N. Coleman, Small 6 (2010) 864–871.
[28] L. Dong, Z. Chen, X. Zhao, et al., Nat. Commun. 9 (2018) 76–84.
[29] A.P. Kauling, A.T. Seefeldt, D.P. Pisoni, et al., Adv. Mater. 30 (2018) 1803784.
[30] Y. Si, E.T. Samulski, Nano Lett. 8 (2008) 1679–1682.
[31] J. Liu, J. Wang, X. Yan, et al., Electrochim. Acta 54 (2009) 5656–5659.
[32] J. Wang, X. Sun, Energy Environ. Sci. 5 (2012) 5163–5185.
[33] C.K. Song, I.S. Yoon, D.D. Kim, Int. J. Pharm. 507 (2016) 102–108.
[34] S. Ahadian, M. Estili, V.J. Surya, et al., Nanoscale 7 (2015) 6436–6443.
[35] T. Bjorkman, A. Gulans, A.V. Krasheninnikov, et al., Phys. Rev. Lett. 108 (2012) 235502.
[36] V.V. Gobre, A. Tkatchenko, Nat. Commun. 4 (2013) 2341–2347.
[37] T. Ming, C. Lin, J. Kong, US2017050856-A1, WO2017031274-A1, 2017.
[38] C.Y. Su, A.Y. Lu, Y. Xu, et al., ACS Nano 5 (2011) 2332–2339.
[39] M. Zhang, R.C. Howe, R.I. Woodward, et al., Nano Res. 8 (2015) 1522–1534.
[40] J. Chen, Y.R. Li, L. Huang, C. Li, G.Q. Shi, Carbon 81 (2015) 826–834.
[41] I.K. Moon, J. Lee, R.S. Ruoff, H. Lee, Nat. Commun. 1 (2010) 73–79.
[42] D. Yang, A. Velamakanni, G. Bozoklu, et al., Carbon 47 (2009) 145–152.
[43] W.C. Du, X.Q. Jiang, L.H. Zhu, J. Mater. Chem. A 1 (2013) 10592–10606.
[44] F.S. Rocha, A.J. Gomes, C.N. Lunardi, S. Kaliaguine, G.S. Patience, Can. J. Chem. Eng. 96 (2018) 2512–2517.